POAC'25
St. John's, Newfoundland and Labrador, Canada

Proceedings of the 28th International Conference on Port and Ocean Engineering under Arctic Conditions
Jul 13-17, 2025
St. John's, Newfoundland and Labrador
Canada

Modelling of thermo-hydrodynamic processes in sea ice ridges

Aleksey Marchenko[1], Knut Hoyland[1,2]
[1] The University Centre in Svalbard, Longyearbyen, Norway
[2] Norwegian University of Science and Technology, Trondheim, Norway

ABSTRACT

Consolidation of ice ridge keels occurs due to the formation of new ice between submerged ice blocks. The consolidation process is of interest for industry because it leads to increasing strength of ice ridges and loads on engineering structures and seabed. In the present paper we consider a set of thermo-hydrodynamic processes inside sea ice ridges influencing the consolidation and discuss mathematical models describing these processes. It includes the formation of new ice at the interface of submerged ice blocks, the rejection of salts into the water during the formation of new ice, mixing of sea water inside ridge keels due to the temperature and salinity gradients, penetration of melt water inside ridge keels from below due to the melting of the keels under the influence of ocean heat flux, and penetration of sea water inside ridge keels from outside under the influence of pressure gradient. In the present paper we derive thermodynamic model equations describing changes in the volumetric solid ice content and water salinity inside unconsolidated rubble similarly to mushy layer model. Then, we compare simulation results obtained by finite element modelling based on the solution of standard heat transfer equation with simulation results obtained using a new model based on the analysis of salinity and thermodynamic equilibrium of water and ice in unconsolidated rubble.

KEY WORDS: ice ridge, heat transfer, salt diffusion, consolidated layer, solid fraction

1 INTRODUCTION

Compression of sea ice influences stress concentrations at the edges of interacting floes, separation of ice blocks from them, and pushing them in the water and on the surface of level ice. Ice rubble extended along specific direction and having smaller dimensions in the transversal direction is called ice ridge (IR). Usually, ice ridges are extended along floes boundaries, but in cases of relatively small diameters of interacting floes IR occupy regions of arbitrary shape. Above water and submerged parts of IR are named sail and keel. Vertical dimension of IR keels is greater than vertical dimension of their sails in 3-5 times (Timco and Burden, 1997). Internal structure of IR is characterized by macro-porosity which is the volume of voids filled with water within unit volume of IR. In practice macro-porosity is calculated using vertical drilling of IR. Macro-porosity in each drilling location is calculated as a ratio of total length of intervals with high drilling speed to total length of the drilling well.
Drilling studies showed the existence of consolidated layer (CL) in upper part of IR keels. Macro-porosity of CL equals zero. The mean value of IR macro-porosity below CL varies from 0.2 to 0.5 with an average value of 0.3, which means that 70% of IR keels are occupied by solid ice and 30% by water (Timco and Burden, 1997). Thickness of CL can be several

times greater the thickness of level ice formed in the same weather conditions. Multiyear IR can be completely consolidated (Kovacs, 1983). Høyland et al (2008), Strub-Klein et al (2009), and Shestov et al (2012) discovered that the second-year ice ridges in the Fram Strait are also completely consolidated in Spring. Marchenko (2022a,b) described completely consolidated first-year IRs observed on Spitsbergen Bank in April 2017-2019.

Ice loads on structures caused by an impact of drifting IR depend on CL thickness. Consolidated ice keels impact into seabed and damage underwater communications and pipelines. Collisions with consolidated fragments of ice rubble of 5-6 m thickness are dangerous for boats of non-ice class. Consolidation effect of IR contributes to the mass balance of drifting ice through the mass of CL layer and mass of unconsolidated rubble. Depending on the number of ice ridges it can be important for the simulations of sea ice dynamics and freshwater balance of Arctic seas. Above mentioned issues explain interest to the modeling of IR consolidation. IR consolidation is explained by mechanical effects of dynamic packing of submerged ice blocks and thermodynamic effects of water freezing between ice blocks inside IR keel. Further, we concentrate on thermodynamic consolidation of submerged IR.

Energy sources for thermodynamic consolidation are atmosphere cooling, cold reserves of submerged ice blocks and chemical potentials of saline ice and water. Effect of atmosphere cooling on the consolidation of IR was considered by Lepparanta et al (1995). It was explained that the latent heat transported away to freeze the unit mass of IR with macro-porosity p equals pL_{sb}, where L_{sb} is the latent heat spent for the melting of submerged ice blocks. According to the Stefan equation the thickness of growing level ice is proportional in quasi-static approximation to $1/\sqrt{L_{si}}$, where L_{si} is the latent heat of sea ice. The ratio of level ice thickness to the CL thickness is proportional to $\sqrt{pL_{sb}/L_{si}} \leq \sqrt{p}$, where p is the macro-porosity of IR keel, and L_{sb} is the latent heat spent for the melting of submerged ice blocks. We assume that $L_{sb} \leq L_{si}$ since the microporosity of submerged ice blocks can be higher the microporosity of floating sea ice. From the data of field measurements Lepparanta et al (CRST, 1995) estimated the initial macro-porosity of $p_0 \approx 0.3$.

Hoyland and Liferov (2005) studied experimentally an influence of cold reserves stored in submerged ice blocks on thermodynamic consolidation of IR on the initial phase after the IR formation. The two IR were formed from artificially broken ice in the Van Mijen Fjord, Svea, in 2002 and 2003 (Liferov and Hoyland, 2004). At the initial phase, the temperature of the submerged ice blocks rises to the freezing point, and the heat flux from the water to the ice blocks is partially converted into latent heat for the formation of new ice and partially used to heat the ice blocks. The initial phase duration was found dependent on the IR dimensions and estimated of four days or smaller for IR with thickness smaller 2.2 m. The ocean heat flux to IR estimated from ice temperature measurements exceeded 200 W/m^2 at the initial phase and then dropped to 2-10 W/m^2. For IR with draft 2.2 m it was measured that CL thickness was 35 cm over the initial phase of 4 days duration, and CL thickness reached 65 cm after 20 days of the experiment. The ratio 35/65=0.54 is greater the ratio of CL thicknesses after 4 and 20 days of consolidation $\sqrt{4/20} \approx 0.45$ following from the Stefan's formula. It means that $\sim 10\%$ of CL thickness formed at the initial phase were related to the release of cold reserves stored in submerged ice blocks.

The release of cold reserves stored in submerged ice blocks influences also a reduction of IR macro-porosity below CL. The effect is estimated from the balance of heat energy of ice $c_i \Delta T(1-p)$ and latent energy for the formation of new ice $L_{sb}\Delta p$ in unit volume of IR. Here c_i is the specific heat capacity of ice, and ΔT is the difference of the freezing point of water and the ice temperature. We found that $\Delta p = c_i \Delta T(1-p)/L_{sb}$. Assuming $c_i \approx 2$ kJ/kg K, $\Delta T \approx 2$°C, $p \approx 0.3$, and $L_{sb} \approx 300$ kJ/kg we found Δp of about few percents. Note, the effect

of porosity reduction can be stronger since the specific heat capacity of saline ice increases with increasing of the temperature in the vicinity of the freezing point (Schwerdtfeger, 1963). The increase in specific heat capacity depends on the ice salinity, and theoretically the specific heat capacity of saline ice tends to infinity as it approaches the freezing point, when the ice salinity tends to zero. The driving force for new ice formation or melting of existing ice inside IR is the difference between ice temperature and freezing point of sea water. In thermodynamic equilibrium chemical potentials of water and ice are the same (Feistel and Hagen, 1998). Difference in the chemical potentials influences phase changes in the system. Advection of fresher water inside IR keel by sea current and mixing of fresher melt water formed at the bottom of IR keel with more saline water inside the keel influence the differences in the chemical potentials leading to ice formation and reduction of IR macro-porosity.

Shestov and Marchenko (2016a) carried out laboratory experiments to demonstrate increasing of ice mass due to cyclic replacements of sea ice cores from fresh water to saline water and back. The fresh and saline waters were at their freezing points. Replacement of ice cores from vessel with saline water to the vessel with fresh water imitated penetration of fresh water inside IR due to advection. Marchenko (2018) carried out laboratory experiments on consolidation of sea ice blocks submerged in water with different temperature. In each experiment two vessels were thermally insulated from below and from the sides by foam plastic, filled by sea ice blocks with temperature -2^{o}C, placed in the cold room and filled with sea water. Initial temperature of sea water in the first vessel was at the freezing point and in the other vessel it was slightly above the freezing point. In the first vessel, IR consolidated due to the cooling only from the surface, and in the second vessel, the consolidation occurred due to the surface cooling and freezing of melt water, replacing seawater inside IR due to convection. It was found that final mass of consolidated rubble was larger in the second vessel. Convective processes inside IR are similar to those in sea ice, where liquid brine trapped in permeable channels and closed brine pockets migrates vertically and changes its volume, temperature and salinity. The micro-porosity of saline ice changes according to the movement of brine (Worster and Jones, 2015). Mathematical models describing ice growth changed from Stefan model considering only thermal diffusion as main physical process responsible for the ice growth to mushy layer model (Wells et al, 2019) considering the impact of salt transport and diffusion on mushy layer growth in addition to thermal diffusion. The permeability of sea ice by brine and Darcy's Law describing migration of brine through the ice are important properties used for the formulation of mushy layer model.

Mathematical models of thermodynamic evolution of IR were subjected similar evolution gradually. Marchenko (2022a, b) formulated one dimensional model where solid ice and water inside unconsolidated rubble (UR) is in thermodynamic equilibrium similarly to mushy layer, while the temperature of CL can be below the freezing point. Standard heat transfer equation was modified to the equation including the volumetric fraction of solid ice, while the temperature was proportional to water salinity according to the condition of thermodynamic equilibrium. The equation of salt diffusion was added to describe changes of sea water salinity inside UR. The standard heat transfer equation was used to describe changes of CL temperature. In the present paper we formulate 3D analog of the model and derive equations of one dimension model by regular method. We compare results of numerical simulations obtained with finite element model based on standard heat transfer realized in Comsol Multiphysics with simulation results obtained with new one-dimensional model. In addition, we analyze the influence of varying temperature of sea water on thermodynamic consolidation of IR.

2 THERMODYNAMIC CONSOLIDATION OF ICE RIDGES IN SEA WATER OF CONSTANT SALINITY

Thermodynamics of sea ice blocks submerged in seawater is described by the equations of thermal conductivity in ice and water and the equation of salt balance in water

$$\rho_i c_i \frac{\partial T}{\partial t} = \nabla(k_i \nabla T), \mathbf{x} \in V_i; \rho_w c_w \frac{\partial T}{\partial t} = \nabla(k_w \nabla T), \frac{\partial S}{\partial t} = \nabla(D \nabla S)\ \mathbf{x} \in V_w, \quad (1)$$

where ρ, c and k denote density, specific heat capacity and thermal conductivity, subscripts i and w are attributed to ice and water, D is is salt diffusivity in water, T and S are temperature and salinity; x, y are horizontal coordinates, z is vertical coordinate, and $\mathbf{x} = (x, y, z)$; $\nabla = (\partial/\partial x, \partial/\partial y, \partial/\partial z)$ is the differential operator, V_i and V_w are the volume filled with ice and water. Sea ice salinity S_i is assumed constant; $\rho_i = 920$ kg/m^3, $k_i = 2.31$ W/m^{o}K.
Movements water due to convection and advection is not considered explicitly in equations (1). Instead, it is assumed that thermal conductivity and salt diffusivity can take effective values $k_w = k_{wt}$ and $D = D_t$ which are much greater the molecular thermal conductivity and salt diffusivity because of turbulent mixing; $\rho_w = 1030$ kg/m^3.
Boundary conditions at moving ice-water interface Σ_{iw} set temperature equal the freezing point T_f (Assur, 1958) and specify heat and salt fluxes

$$T = T_f(S) \equiv -\alpha S, \alpha = 54.9°\text{C}, \quad (2)$$

$$\rho_i L_i v_{\Sigma,n} = k_i \frac{\partial T}{\partial n}\Big|_{\mathbf{x}\in\Sigma_{iw}-0} - k_w \frac{\partial T}{\partial n}\Big|_{\mathbf{x}\in\Sigma_{iw}+0}, \quad (3)$$

$$-\rho_w D \frac{\partial S}{\partial n}\Big|_{\mathbf{x}\in\Sigma_{iw}+0} = (\rho_w S - \rho_i S_i) v_{\Sigma,n}, \quad (4)$$

where $v_{\Sigma,n}$ is the interface velocity in projection on unit normal $\mathbf{n}$ directed from ice to water, and L_i is the latent heat.
Boundary condition at the surface of CL is the heat budget (Makshtas, 1991)

$$-k_i \frac{\partial T}{\partial n} = \rho_a c_a St V_a (T_s - T_a), z = h_s, \quad (5)$$

where $\rho_a = 1.37$ kg/m^3 is air density, $c_a = 1$ kJ/(kg^{o}K) is specific heat capacity of air, $St = 0.0017$ is the Stanton number, V_a is wind speed, and T_a is air temperature at 10 m height.
Numerical simulations of equations (1) with boundary conditions (2)-(5) meet technical problems when geometry of ice volume V_i is complicated. The problems are partially overcome if water salinity is assumed to be a constant. In this case the heat transfer equations in water and ice and boundary conditions (2) and (3) are satisfied by the consideration of generalized heat transfer equation

$$(\rho c + \rho_i L_i \delta(T - T_f)) \frac{\partial T}{\partial t} = \nabla(k \nabla T), \mathbf{x} \in V_i + V_w, \quad (6)$$

where $\delta(T - T_f)$ is the Dirac delta-function, and the coefficients ρ, c, and k are density, specific heat capacity and thermal conductivity of water by $\mathbf{x} \in V_w$ and ice by $\mathbf{x} \in V_i$. Equation (6) supports that ice occupies the region with $T < T_f$, and water occupies the region with $T > T_f$. The ice-water interface coincides with isothermal surface $T = T_f$. The ridge sail and the 20 cm thick snow layer located at $y > 50$ cm consist respectively of 80% and 30% ice.

Numerical procedure of solution of equation (6) was realized in finite element software Comsol Multiphysics. The procedure includes smoothing of the delta-function over phase transition interval of temperature ΔT around the freezing point $T = T_f$. Figure 1 shows an example of simulation results after 80 days of thermodynamic evolution of IR with initial macro-porosity of 30% and initial temperature of submerged ice blocks of -5 ºC. The initial configuration of ice blocks is shown in Fig. 1a. The freezing point was set to -1.94 ºC and phase transition interval was 0.05ºC. It means that we may tell, that regions, where the temperature is below -1.965ºC and above -1.915 ºC correspond to ice and water, and based on the computer simulations we can't conclude what is the phase within the temperature interval between -1.965ºC and -1.915ºC. We used turbulent thermal conductivity of water $k_{wt} = 1000$ W/(mºK).

In this paper we consider thermodynamic evolution of IR shown in Fig. 1a. The trajectory of IR drift shown in Fig. 1b was constructed using the data of numerical simulations of ocean dynamics and ice drift in the Barents Sea (Marchenko et al., 2016). The bottom of level ice is at $y = 0$. The ice drifted along this trajectory for 50 days. The air and water temperature along the trajectory used in the simulations are shown in Fig. 2 versus time. The wind velocity along trajectory 3 was also taken from the simulations. We assumed that after 50 days the air temperature, water temperature and wind speed were constant for 30 days. Figure 3 shows temperature distribution inside the computational domain obtained after 80 days of the thermodynamic evolution of the IR. Colors in Fig. 3 are used to show boundaries between dark blue and light blue areas corresponding the isotherm -1.965ºC and green and yellow areas corresponding to the isotherm -1.915ºC. Boundary between green and light blue areas corresponds to the freezing point.

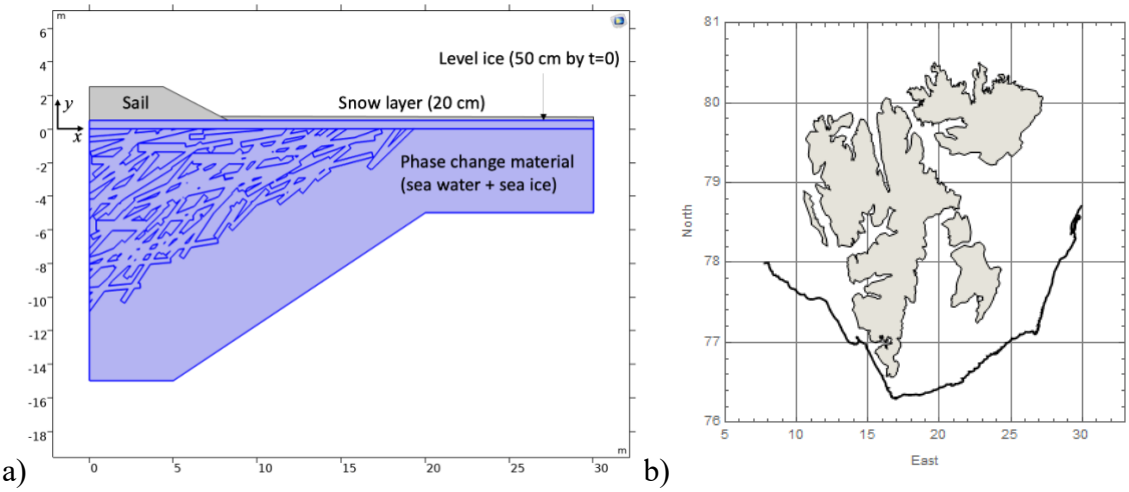

a) b)

Figure 1. (a) Computational domain in Comsol Multiphysics, (b) simulated trajectories of IR drift.

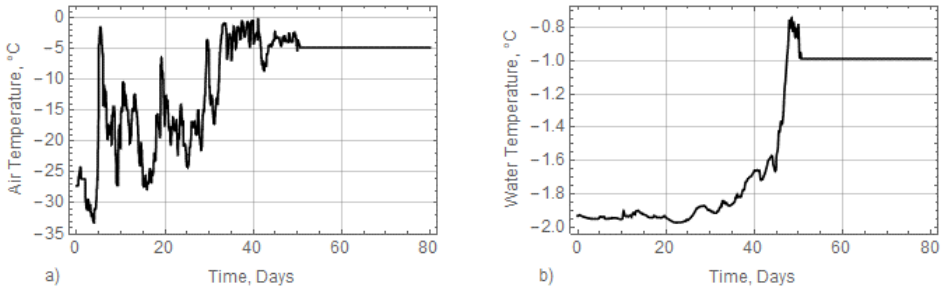

Figure 2. Air (a) and water (b) temperatures used in the simulations.

One can see that although the program calculated temperature distribution it is impossible to distinguish water and ice inside IR and make any conclusion on the macro-porosity. We may tell that IR melted from below and the draft became smaller on 2 m. It is necessary to use transition interval smaller 0.05°C what has little physical sense because natural fluctuations of sea water temperature can be greater this value. We may also see that salinity is a better indicator of the ice-water interface than temperature, as water salinity is around 30 ppt, while warm sea ice salinity is less than 15 ppt. Therefore, there is a practical reason to consider a salinity based model of thermodynamic consolidation of IR that assumes thermodynamic equilibrium of water and ice within unconsolidated rubble.

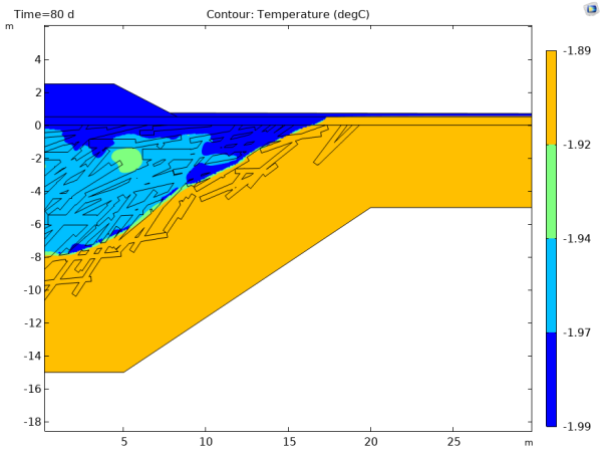

Figure 3. Boundaries between dark blue and light blue areas correspond to the isotherm -1.965°C, green and yellow areas correspond to the isotherm -1.915°C. Boundary between green and light blue areas corresponds to the freezing point. Yellow and dark blue colors specify regions where the ice temperature is higher -1.915°C and lower -1.965°C.

3 THERMODYNAMIC CONSOLIDATION OF ICE RIDGES IN SEA WATER OF VARIABLE SALINITY

To model long-term thermodynamic evolution of IR we assume that it consists of CL and UR below the CL (Fig. 4). Low boundaries of CL and UR are described by the formulas

$$z = -h_{CL}(x, y, t), \quad z = -h_{UR}(x, y, t), \tag{7}$$

where x and y are the horizontal coordinates, and t is time. The CL is located at $z \in (0, -h_{CL})$, and UR occupies the region $z \in (-h_{CL}, h_{UR})$. CL has properties similar solid sea ice. UR consists of seawater and solid ice blocks with constant salinity $S_i = const$.
Temperature distribution inside CL is described by heat transfer equation (1) similar to the heat transfer equation in solid ice. Sea ice salinity S_i is assumed constant inside UR. Accounting for diffusion and latent heat released by internal phase changes, conservation of heat energy for UR yields

$$\rho_i L_i \frac{\partial \phi}{\partial t} = \langle \rho c_p \rangle \frac{\partial T}{\partial t} - \nabla(\langle k \rangle \nabla T), z \in (-h_{CL}, h_{UCR}), \tag{8}$$

where ϕ is the volumetric fraction of solid ice inside UR, L_i is the latent heat, $\langle \rho c_p \rangle = \phi \rho_i c_i + (1 - \phi)\rho_w c_w$, and $\langle k \rangle = \phi k_i + (1 - \phi)k_w$.
The corresponding phase-weighted equation for conservation of solute is

$$\frac{\partial}{\partial t} S_{UR} = \nabla(\rho_w(1-\phi)D\nabla S), z \in (-h_{CL}, h_{UCR}), \tag{9}$$

where $S_{UR} = \rho_w(1-\phi)S + \rho_i \phi S_i$ is the salinity of unit volume of UR.
Boundary condition at the surface of CL is heat budget (5). Boundary conditions at the bottom of CL by $z = -h_{CL}$ consist of energy balance and salt balance

$$\rho_i(1-\phi)L_i v_{CL,n} = k_i \frac{\partial T}{\partial n}\Big|_{z=-h_{CL}+0} - \langle k \rangle \frac{\partial T}{\partial n}\Big|_{z=-h_{CL}-0}, \tag{10}$$

$$-\rho_w(1-\phi)D\frac{\partial S}{\partial n}\Big|_{z=-h_{CL}-0} = (1-\phi)(\rho_w S - \rho_i S_i)v_{CL,n}, \tag{11}$$

where **n** is outward unit normal to the bottom of CL, and $v_{CL,n}$ is normal velocity of CL bottom (Fig. 4). Equation (10) sets that the difference of the heat fluxes from CL and UR to the bottom of CL spends for the formation of new ice from the water trapped in UR. The rate of ice volume formation is $v_{CL,n}\delta s$, where δs is an infinitesimal area on the bottom of CL. The mass of salts in this volume before freezing is $\rho_w S v_{CL,n}\delta s dt$ and after freezing it is $\rho_i S_i v_{CL,n}\delta s dt$. Formula (11) sets that difference between these masses equals to the flux of salts into UR.
Boundary conditions at the bottom of UR by $z = -h_{UR}$ also expressed by energy balance and salt balance

$$\rho_i \phi L_i v_{UR,n} = -Q_w + \langle k \rangle \frac{\partial T}{\partial n}, \tag{12}$$

$$-\rho_w(1-\phi)D\frac{\partial S}{\partial n} = -\phi(\rho_w S - \rho_i S_i)v_{UR,n} + \rho_w u_* C_s us(S - S_{sw}), \tag{13}$$

where **n** is outward unit normal to the bottom of UR, $v_{UR,n}$ is normal velocity of UR bottom, Q_w is the heat flux from ocean, $u_* = 1$ cm/s is the turbulent velocity scale (McPhee, 1992), $C_s \approx 2 \cdot 10^{-4}$ is the diffusion coefficient (McGuiness, 2009), S_{sw} is water salinity below IR, and $us(x)$ is unit step function equal 0 by $x < 0$ and 1 by $x > 0$. Equation (12) sets that the difference of the heat fluxes from ocean and UR spends for the melting of ice at the bottom of UR. Equation (13) determines the salt flux at the bottom of UR due to replacement of sea water volume with the same melt water volume inside the rubble. The last term in the right part of (13) describe turbulent diffusion of salts from UR into water when the salinity of UR is greater water salinity below UR (McGuiness, 2009).

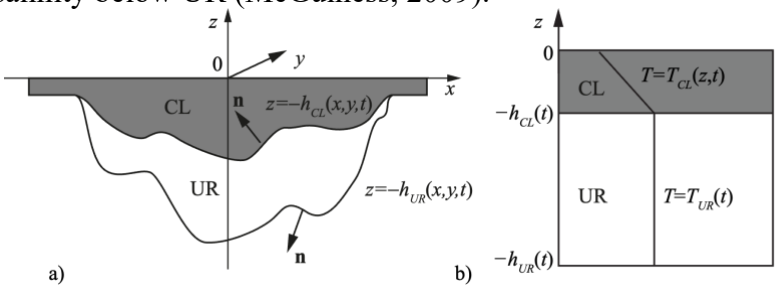

Figure 4. Schematic of ice rubble structure in 3D model (a) and 1D model (b).

Further we derive the equations of heat and salt balance integrated over the volume of UR using formula for the differentiation of an integral over a moving volume V bounded by the surface Σ

$$\frac{d}{dt}\int_V f dV = \int_V \frac{\partial f}{\partial t} dV + \int_\Sigma f v_n d\Sigma, \tag{14}$$

where v_n is the normal velocity of the surface Σ. To apply this formula to equation (3) we write

$$\langle \rho c_p \rangle \frac{\partial T}{\partial t} = \frac{\partial (\langle \rho c_p \rangle T)}{\partial t} - T(\rho_i c_i - \rho_w c_w) \frac{\partial \phi}{\partial t}. \quad (15)$$

The second term in the right part of (15) is omitted after substitution of (15) into (8) since

$$\alpha S |\rho_i c_i - \rho_w c_w| \ll \rho_i L_i. \quad (16)$$

Using formula (14), inequality (16) and boundary conditions (10)-(13) the heat budget and salt budget equations integrated over UR volume are written as follows

$$\frac{d}{dt}\int \left(\rho_i L_i \phi - \langle \rho c_p \rangle T\right) dV = \int_{\Sigma_{CL}} \left(\rho_i L_i \phi - \langle \rho c_p \rangle T\right) v_{CL,n} d\Sigma + \int_{\Sigma_{CL}} \left[\rho_i (1-\phi) L_i v_{CL,n} - k_i \frac{\partial T}{\partial n}\Big|_{z=-h_{CL}+0}\right] d\Sigma + \int_{\Sigma_{UR}} \left(\rho_i L_i \phi - \langle \rho c_p \rangle T\right) v_{UR,n} d\Sigma - \int_{\Sigma_{UR}} \left[\rho_i \phi L_i v_{UR,n} + Q_w\right] d\Sigma, \quad (17)$$

$$\frac{d}{dt}\int S_{UR} dV = \int_{\Sigma_{CL}} [S_{UR} - (1-\phi)(\rho_w S - \rho_i S_i)] v_{CL,n} d\Sigma + \int_{\Sigma_{UR}} [S_{UR} + \phi(\rho_w S - \rho_i S_i)] v_{UR,n} d\Sigma. \quad (18)$$

Equations (17) and (18) are modified to more compact form when the bottoms of CL and UR are the horizontal planes described by the equations $z = -h_{CL}(t)$ and $z = -h_{UR}(t)$. Normal velocities are equal $v_{CL,n} = -dh_{CL}/dt$ and $v_{UR,n} = dh_{UR}/dt$. Assuming $\phi = \phi(t)$ and $S = S(t)$ and using (2) we derive from (17) and (18) two equations for calculation of $\phi(t)$ and $S(t)$

$$\rho_i L_i (h_{UR} - h_{CL}) \frac{d\phi}{dt} + \alpha \langle \rho c_p \rangle (h_{UR} - h_{CL}) \frac{dS}{dt} = = -k_i \frac{\partial T}{\partial n}\Big|_{z=-h_{CL}+0} - \rho_i (1-\phi) L_i \frac{dh_{CL}}{dt} - Q_w + \rho_i \phi L_i \frac{dh_{UR}}{dt}, \quad (19)$$

$$(h_{UR} - h_{CL}) \frac{dS_{UR}}{dt} = = (1-\phi)(\rho_w S - \rho_i S_i) \frac{dh_{CL}}{dt} + \phi(\rho_w S - \rho_i S_i) \frac{dh_{UR}}{dt} + \rho_w u_* C_s u s (S - S_{sw}). \quad (20)$$

where $S_{UR} = \rho_w (1-\phi) S + \rho_i \phi S_i$. Boundary conditions (10) and (12) are modified now to two equations for the finding of $h_{CL}(t)$ and $h_{UR}(t)$

$$\rho_i (1-\phi) L_i \frac{dh_{CL}}{dt} = -k_i \frac{\partial T}{\partial n}\Big|_{z=-h_{CL}+0}, \quad (21)$$

$$\rho_i \phi L_i \frac{dh_{UR}}{dt} = -Q_w, \quad (22)$$

with assumption $\partial T/\partial n|_{z=-h_{CL}+0} \le 0$ and $Q_w \ge 0$.

System of equations (19)-(22) is similar the equations derived in (Marchenko, 2022a, 2022b). The difference is in the parametrization of the heat fluxes at the boundaries of UR in equation (19). In above mentioned papers the right part of equation (19) is replaced with $-\phi k_i \partial T/\partial n|_{z=-h_{CL}+0} + (1-\phi) Q_w$ to specify different way of the splitting of heat fluxes spent for phase changes and heat transfer in ice at the bottom of CL and in water at the bottom of UR. We believe that equation (19) is more correct, since it clearly agreed with the growth and melt of ice at the boundaries of UR.

The heat flux at the surface of CL can be estimated assuming linear profile of the temperature inside CL ignoring the thermal inertia (Fig. 4b). It leads to the formula valid in the entire CL

$$\frac{\partial T}{\partial z} = \frac{T_s + \alpha S}{h_{CL}}, \tag{23}$$

where T_s is the temperature of CL at $z = 0$. The surface temperature T_s is related to the heat flux at the surface by formula (5).

The heat flux from ocean was determined by the formula (McPhee, 1992)

$$Q_w = \rho_w c_w u_* \Phi_T^{-1}(T_w - T_{UR}), \tag{24}$$

where $\Phi_T = 200$ is the reciprocal heat transfer coefficient.

4 RESULTS OF NUMERICAL SIMULATIONS

Numerical simulations of equations (19)-(22) was carried out for the air and water temperatures, and wind speed calculated along trajectory of ice drift shown in Fig. 1b, i.e. we used boundary conditions similar the simulations with Comsol Multiphysics discussed in Section 2. Simulations were carried out with two initial values of the volumetric fraction of solid ice ϕ_0 equal 0.7 and 0.8 for 80 days. The initial draft of IR was 10 m, and the initial thickness of CL was 1 m. The initial temperature of IR was -1.95ºC. Simulation results are shown in Fig.5 versus time. The thickness of CL was growing monotonically in time and reached 2.5 m with $\phi_0 = 0.7$ and 3 m with $\phi_0 = 0.8$ to the end of the simulations. IR draft monotonically decreased and reached 6 m with $\phi_0 = 0.7$ and 7.5 m with $\phi_0 = 0.8$ to the end of the simulations. The volumetric fraction of solid ice ϕ in UR monotonically decreased and reached 0.36 with $\phi_0 = 0.7$ and 0.6 with $\phi_0 = 0.8$ to the end of the simulations. UR with $\phi = 0.36$ will be probably destroyed due to influence of sea currents, while UR with $\phi = 0.6$ could relatively stable under actions of sea currents.

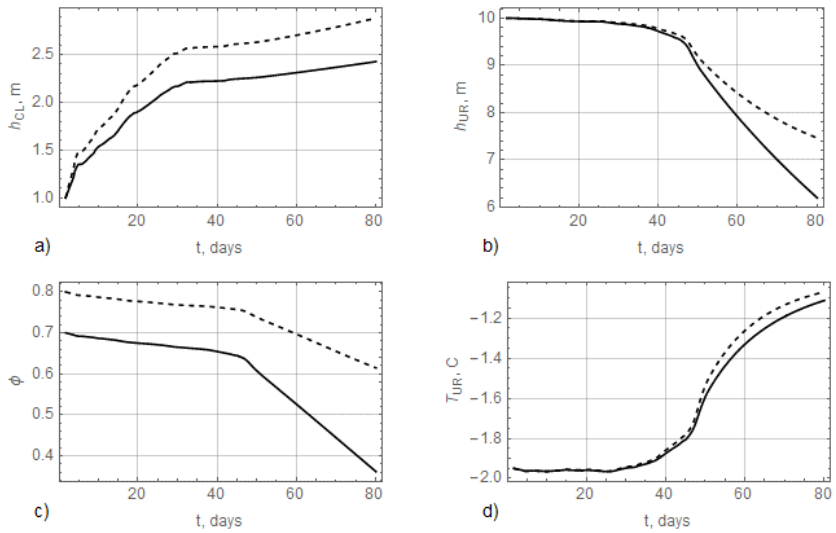

Figure 5. Simulation results obtained with $\phi_0 = 0.7$ (solid lines) and $\phi_0 = 0.8$ (dashed lines) for IR drifting along trajectory shown in Fig. 1b: (a) Thicknesses of CL (a), drafts of IR (b), the volumetric fractions of solid ice in UR (c), temperature of UR (d) versus time.

Numerical simulations of equations (19)-(22) was carried out for constant surface temperature of IR $T_s = -5℃$ with constant and varying temperatures of sea water T_w below IR. Figure 6a shows the constant temperature $T_{w,1} = -1.65℃$ and temperature $T_{w,2}$ changing periodically between -1.9ºC and -1.4ºC with period of about 50 days. Simulations were performed with two initial values of the volumetric solid ice fraction $\phi_0 = 0.7$ and $\phi_0 = 0.8$. Simulations

showed that the volumetric fraction of solid ice ϕ decreased when $T_w = T_{w,1}$ and increased when $T_w = T_{w,2}$ for both values of ϕ_0 (Fig. 6b). Drafts of IR decreased monotonically ($dh_{UR}/dt \leq 0$) in all considered cases. The mean melting rate of UR was larger when the water temperature varied (Fig. 6c). CL thickness monotonically increased in all considered cases, but freezing rates were higher when IR drifted in the water with changing temperature (Fig. 6d). Macro-porosity of UR with $\phi_0 = 0.8$ reached 0.1 after 350 days of the consolidation. This means that this IR with a draft of 7.6 m is completely consolidated, since the UR macro-porosity of 0.1 is similar the micro-porosity of submerged sea ice blocks.

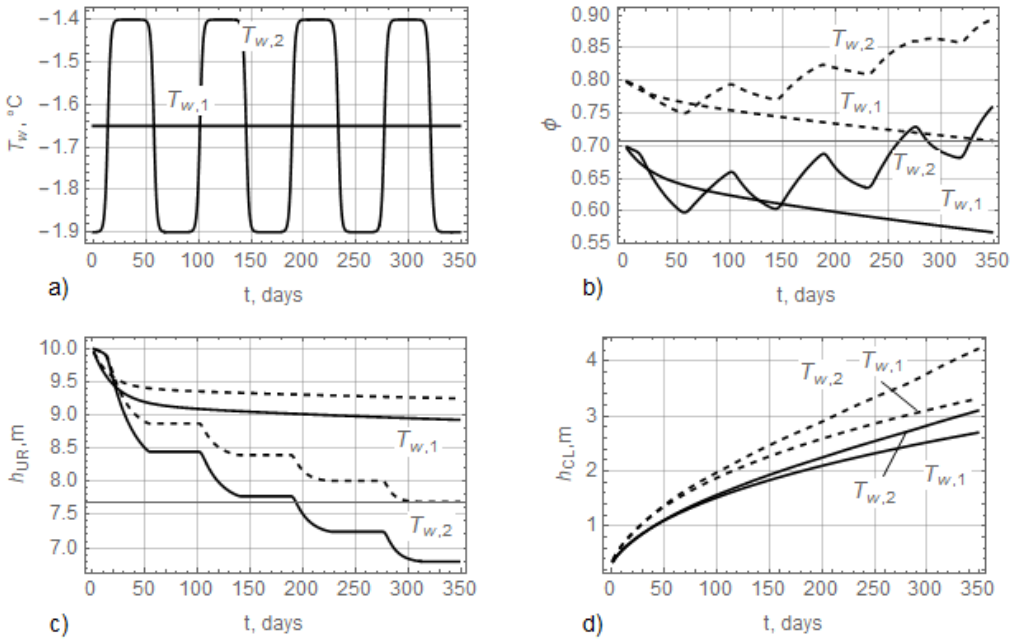

Figure 6. Simulation results obtained with $\phi_0 = 0.7$ (solid lines) and $\phi_0 = 0.8$ (dashed lines), constant temperature at IR surface -5°C and water temperatures at IR bottom $T_{w,1}$ and $T_{w,2}$ (a). The volumetric fractions of solid ice in UR (b), drafts of IR (c), and thicknesses of CL (d) versus time.

5 CONCLUSION

Modeling the thermodynamic evolution of IR by the finite element method has for relatively long time encountered the technical problem of distinguishing between water and ice when using the generalized heat transfer equation. The length of temperature transition interval in the model tends to zero with increasing of the simulation time if distinguishing between water and ice is taken by the temperature criterion. Salinity based criterion is more realistic for distinguishing between water and ice if ice and water temperatures are similar.

We formulated model of the thermodynamic evolution of IR consisting of consolidated layer (CL) and unconsolidated rubble (UR). Temperature changes in CL are described by the standard heat transfer equation. The evolution of UR is described by modified heat transfer equation depending on the volumetric fraction of solid ice and the equation of salt diffusion. The model assumes that ice and water are in thermodynamic equilibrium inside UR. Solving these equations we found the dependencies of CL temperature, the volumetric fraction of solid ice and water salinity of UR from time. The movement of the bottoms of CL and UR is calculated from the boundary conditions.

Model equations and boundary conditions were simplified for one dimensional IR which properties don't change in horizontal directions. A system of four ordinary differential equations was derived to describe temporal evolution of the volumetric fraction of solid ice

and water salinity of UR, the thickness of CL and the draft of IR. The equations account explicitly energy fluxes for phase changes at the boundaries of CL. Numerical simulations demonstrated reasonable evolution of IR characteristics for simulation times of 80 days and 350 days. Simulations showed that changes of sea water temperature in time increase consolidation rate of IR.

ACKNOWLEDGEMENTS

This work has been supported by the NFR sponsored project 326834: Risk of sea ice and icebergs for field development in the Southwestern Barents Sea (RareIce).

REFERENCES

Assur, A., 1958. Composition of sea ice and its tensile strength, in: Arctic sea ice; conference held at Easton, Maryland, February 24– 27, 1958, Vol. 598 of Publs. Natl. Res. Coun. Wash., Washington, DC, US,106–138.

Feistel, R., Hagen, E., 1998. A Gibbs thermodynamic potential of sea ice. Cold Reg. Sci. Technol. 28 (2), 83–142.

Hoyland, K.V., Liferov, P., 2005. On the initial phase of consolidation. Cold Reg. Sci. Technol. 41, 49–59.

Høyland, K.V., Barrault, S., Gerland, S., Goodwin, H., Nicolaus, M., Olsen, O.M., Rinne, E., 2008. The consolidation in second- and multi-year sea ice ridges. Part I: Measurements in earlier winter. In Proceedings of the 19th IAHR International Symposium on Ice, Vancouver BC, Canada, 6–11 July 2008; pp. 1439–1449.

Kovacs, A.,1983. Characteristics of multi-year pressure ridges. In Proceedings of the POAC'83, Helsinki, Finland, 5–9 April 1983, Volume 2, pp. 173–182.

Lepparanta, M., Lensu, M., Koslof, P., Veitch, B., 1995. The life story of a first-year sea ice ridge. Cold Reg. Sci. Technol. 23, 279–290.

Makshtas, A.P., 1991. The Heat Budget of Arctic Ice in the Winter. Int. Glac. Soc., Cambridge. 77 pp.

McGuiness, M.J., 2009. Modeling of sea ice growth. ANZIAM J., 50, 306–319.

McPhee, M.,G., 1992. Turbulent heat flux in the upper ocean under sea ice. J. Geoph. Res., 97(NC4): 5365-5379.

Marchenko, N., Marchenko, A., 2017. Investigation of large ice rubble field in the Barents Sea. POAC17-097.

Marchenko, A., Diansky, N., Fomin, V., Marchenko, A., Ksenofontova, D., 2016. Consolidation of Drifting Ice Rubble in the North-West Barents Sea. Proc. of the 23rd IAHR Symposium on Ice, Ann Arbor, Michigan, paper 4868538.

Marchenko, A., 2018. Influence of the water temperature on thermodynamic consolidation of ice rubble. Proc. of the 24th IAHR Symposium on Ice, Vladivostok, paper 18-005.

Marchenko A.V., 2022a. Thermo-hydrodynamics of sea ice rubble. J. Tuhkuri and A.Polojarvi (Eds), IUTAM Symposium on Physics and Mechanics of Sea Ice, IUTAM Bookseries 39, Springer Nature Switzerland AG, 203-223.

Marchenko, A., 2022b. Modeling of thermodynamic consolidation of sea ice ridges drifting in the water with changing temperature. J. Marine Science and Engineering. 10, 1858.

Schwerdtfeger, P., 1963. The thermal properties of sea ice. J. Glaciol. 4 (36), 789–807.

Shestov, A., Høyland, K.V., Eceberg, O.C., 2012. Morphology and physical properties of old sea ice in the Fram Strait 2006–2011. In Proceedings of the 21st IAHR International Symposium on Ice, Dalian, China, 11–15 June 2012; Volume 52.

Shestov, A.S., Marchenko, A.V., 2016a. The consolidation of saline ice blocks in water of varying freezing points: Laboratory experiments and computer simulations. Cold Regions Science and Technology, 122, 71-79.
Shestov, A.S., Marchenko, A.V., 2016b. Thermodynamic consolidation of ice ridge keels in water at varying freezing points. Cold Regions Science and Technology, 121, 1-10.
Strub-Klein, L., Barrault, S., Goodwin, H., Gerland, S., 2009. Physical properties and comparison of first- and second-year sea ice ridges. In Proceedings of the POAC'09, Luleå, Sweden, 9–12 June 2009; Volume 117.
Timco, G.M., Burden, R.P., 1997. An analysis of the shapes of sea ice ridges. Cold Reg. Sci. Technol. 25, 65–77.
Wells, A.J., Hitchen, J.R., Parkinson, J.R.G., 2019. Mushy-layer growth and convection, with application to sea ice. Phil. Trans. R. Soc. A 377: 20180165.
Worster, M.G., Rees Jones, D.W., 2015. Sea-ice thermodynamics and brine drainage. Phil. Trans. R. Soc. A 373: 20140166.